Journal of Ocean Engineering and Marine Energy (2024) 10:155–174
https://doi.org/10.1007/s40722-023-00305-x

RESEARCH

Sensitivity of turbulence parameters to tidal energy converter loads in BEM simulations

Alyona Naberezhnykh[1,2] · David Ingram[1] · Ian Ashton[2] · Calum Miller[3]

Received: 27 March 2023 / Accepted: 18 October 2023 / Published online: 13 December 2023
© The Author(s) 2023

Abstract
Renewable energy is playing an increasingly central role in the global energy supply due to decarbonisation and energy security aims. A vital aspect of renewable energy systems will be the predictability of the energy source, something that tidal stream energy can provide. The tidal sites suitable for energy extraction are by their nature turbulent, creating variations in the tidal energy converter (TEC) loads and affecting device durability. Developers use Blade Element Momentum (BEM) models to predict loading and improve designs of TECs. To simulate turbulence effects within these models, a synthetic flow field is generated using a combination of measured and assumed parameters. Inaccuracies in these parameters can lead to uncertainties in the simulated loads. This study investigates the sensitivity of turbulence characteristics to loads using a commercial BEM software. Variability in parameters shows a profound impact on the loads. Varying turbulence intensity resulted in a 90% change in fatigue loads for intensities ranging 2–24%. Length-scales showed a 49% decrease in loads across the range tested (5–70 m). A coherent flow field increased loads by 45% compared to a non-coherent flow. Hub-bending loads varied by 30% between different shear profiles, however varying the standard deviation profiles did not show notable effects. The results from this study emphasise the necessity for accurate turbulence parameter inputs to reduce uncertainty in device load modelling. It also highlights the importance of using realistic shear profiles as well as appropriate coherence models.

Keywords Tidal energy converter · Fatigue load · Turbulence · Modelling

1 Introduction

Renewable energy is playing an increasingly central role in global energy supply due to the twin aims of decarbonisation and energy security. Tidal energy is distinctive amongst renewable energy technologies in that it is highly predictable, which means it can fill a key role in a renewables-based energy mix. In the UK, 11.5 GW of tidal stream energy could feasibly be deployed making up 11% of the current electricity demand (Frost 2022). Full-scale tidal energy converters (TECs) such as the Orbital Marine O2 floating turbine, have already been deployed at test sites and have demonstrated the potential of the technology. New UK government support for 53MW of tidal stream development has recently been secured from the CfD Allocation Round 5 (DESNZ 2023), which is a key step in integrating tidal energy arrays into the national energy infrastructure over the coming years.

For tidal energy to fulfil a role within large scale energy systems, it will need to continue to demonstrate reliability for new commercial projects. The tidal sites suitable for energy extraction are by their nature energetic and turbulent, such unsteady flows create variations in power and device loading (Clark et al. 2015; Milne et al. 2016; Scarlett and Viola 2020). Fluctuating loads can result in fatigue or extreme loading exceeding the ultimate strength of components and potentially causing damage to devices (Smyth 2019). As tidal current and marine hydro-kinetic energy converters start to be deployed in arrays and rotor sizes are set to grow, it is critical to better understand how tidal energy devices perform under various levels of turbulence. As such, the accuracy of methods to predict device loads based on the conditions measured at deployment sites is of increasing importance.

✉ Alyona Naberezhnykh
alyona.naberezhnykh@ed.ac.uk

1 School of Engineering, University of Edinburgh, Edinburgh EH9 3JW, UK

2 College of Engineering Mathematics and Physical Sciences, University of Exeter, Penryn TR10 9FE, UK

3 Hydrodynamics Department, Orbital Marine Power Ltd., Kirkwall TR10 9FE, UK

There are two broad modelling approaches for analysing hydrodynamic effects of turbulent flows on a tidal turbine, Blade Element Momentum Theory (BEM) and Computational Fluid Dynamics (CFD) models (Ortega et al. 2020). BEM theory is a well-established approach for analysing conventional horizontal-axis rotors, used for both wind and tidal applications. BEM models enable simulations of device loadings at low computational cost and hence are used in turbine design optimization. They have been successfully applied to predict the performance of TECs (El-Shahat et al. 2020; Parkinson and Collier 2016; Perez et al. 2020). CFD models enable a more detailed study of device-flow interactions. However, the significant increase in complexity and computational cost can make them unsuitable as design tools, for example when many simulations are required to study various flow conditions.

To simulate turbulence effects on devices, BEM models require a turbulent flow field as input. A synthetic flow field can be generated using a combination of parameters derived from physical observations and theoretical assumptions. Recreating a realistic flow is non-trivial, uncertainties can arise when using analytical or empirical models or inaccurate measurements. An important consideration is which input turbulence parameters contribute the most to device loads and hence where higher precision is required.

A number of modelling and experimental investigations have tried to relate turbine loads to turbulence characteristics. A finding that has been consistent is that turbulence intensity, I - a measure of the overall fluctuations in the flow - is an important parameter. Experimental investigations by Mycek et al. (2014) and Blackmore et al. (2016) have demonstrated a sensitivity of the load fluctuations to the turbulence intensity in the flow. Using real site data as input to BEM models, Perez et al. (2022a) and Mullings and Stallard (2021) also found strong correlations of I to load fluctuations. Although studies agree that turbulence intensity is important, the relative importance of other parameters is not well understood.

Shear profiles describe the mean velocity throughout the water column, creating a non-uniform inflow velocity gradient across a turbine's rotor. This will cause eccentric bending moments (Nevalainen et al. 2016), with implications for turbine loading. CFD studies by McNaughton et al. (2013) and Nevalainen et al. (2016) observed large fluctuations in the loading coefficients for varying shear profiles. Clark et al. (2015) also observed large differences in fatigue loads between various shear profiles and Perez et al. (2022a) found increased load standard deviations when the rotor was located closer to the seabed—associated with the pronounced shear. In analysing the relative importance of shear profiles for wind applications, Robertson et al. (2019) concluded that wind shear effects can be equal to or even higher than turbulence intensity. The relative importance of the two parameters is not known for tidal applications.

Using tank experiments, Blackmore et al. (2015) found a larger increase in load fluctuations from increasing integral length scales (size of the most energetic turbulent eddies) than from increasing turbulence intensity. Conversely, Milne et al. (2010) and Perez et al. (2022a) both conducted BEM studies using different models and found load standard deviations were substantially more sensitive to turbulence intensities than the integral length-scales. In analysing power fluctuations of a turbine in real-sea conditions, Sentchev et al. (2020) found these to be correlated with the length-scales and the strongest impact of turbulence on power generation was detected when the integral length-scale was similar to turbine size. Based on previous findings (Blackmore et al. 2015; Sentchev et al. 2020; Hu et al. 2018), it is likely that the integral length-scale impacts loads when it is in the order of the rotor size, albeit there is disagreement on the relative importance of this parameter.

It is also important to understand if there is a benefit to making synthetic flows more realistic. Stochastic models such as TurbSim or Tidal Bladed reconstruct the velocity time series based on spectral and statistical flow characteristics and make a number of simplifications. One such simplification is to assume a constant standard deviation throughout the water column. In real flows, standard deviation will vary across the water column (Naberezhnykh et al. 2023b), but the effect of this on loads has not been investigated. Moreover, it is understood that without proper consideration of coherency in the flow, the loads are unlikely to be accurately resolved (Naberezhnykh et al. 2023b). Coherency is defined as the spatial correlation of fluctuations at each frequency. It can be added into stochastic flow models by explicit definition of the coherence function. In a sensitivity study of TurbSim parameters (for wind applications) Robertson et al. (2019) found that coherency and veer both impacted load estimates, although secondary to parameters such as shear or turbulence intensity. No such investigations have been carried out for tidal applications.

Where modelling studies focus on replicating specific flow conditions using a combined set of parameters rather than varying each parameter separately, it is difficult to decouple the effects of the individual turbulence characteristics. Moreover, experimental studies such as those using static grids in tanks are normally limited by the range of conditions that can be recreated. This work investigates the sensitivity of key turbulence parameters, which are used as inputs to BEM models, to the resulting device loads. Unlike previous studies, each parameter is varied individually, allowing to study the separate effects of varying shear profiles, turbulence intensity, length-scales, standard deviation profiles and coherence. The comprehensive study provides a comparative view of the importance of key turbulence parameters.

2 Methods

2.1 Models

The commercially available design code Tidal Bladed from DNV (DNV 2023) is used in this study to simulate device loads. Tidal Bladed is an adaptation of Bladed for wind turbines and has undergone its own experimental validation programme (Milne et al. 2010). Although Tidal Bladed can be used to generate turbulent flow fields, here we use TurbSim (NREL 2023), which functions by the same principles but allows more flexibility to vary turbulence parameters. TurbSim is an open-source turbulence simulator developed by NREL. It enables the addition of user input length-scale, standard deviation and shear profiles as well as varying coherence. It can output the flow fields as *Bladed-Style Full-Field Files*, which are compatible with Tidal Bladed (Jonkman and Kilcher 2012).

The principles of generating a 3-D turbulent flow field are based on the spectral method (Veers 1988), in which separate velocity time histories are computed for several points across the rotor plane. Each point has predefined single-point spectral characteristics and each pair of points has predefined coherence characteristics (Milne et al. 2010). The time histories are scaled according to the mean velocity, which varies with depth according to the specified shear profile and turbulence intensity. This is illustrated in Fig. 1.

Tidal Bladed uses a multi-body structural dynamic formulation to compute loads and deflections on the turbine support structure and rotor due to hydrodynamic loading (Parkinson and Collier 2016). Lift and drag coefficients are provided by the user and are applied to determine the hydrodynamic forces within the blade elements. Suitable corrections are applied to model the number of blades, the blade definition and flow unsteadiness. The formulation also includes corrections for flow blockage, hub and tip loss models, dynamic inflow/wake model and stall models (Khairuzzaman 2016).

2.2 Turbulence parameters for testing

Figure 1 summarises the inputs required for generating a turbulent flow field in TurbSim, showing that the key parameters for load sensitivity tests are:

- turbulence intensity
- length-scales
- shear profile
- standard deviation profile
- coherence

The tests are designed so that only one parameter is varied at a time, keeping all other characteristics the same. This allows to study the effects of each turbulence parameter variability, allowing a comparison of the sensitivities. This will help to understand which parameters are the most critical and hence need to be measured directly rather than estimated. The ranges were selected to yield realistic combinations of parameters, as described in this section. The loads are reported as a percentage change relative to the maximum value in the test set, allowing to see the relative effect of each parameter variability.

Test 1: turbulence intensity

The streamwise turbulence intensity is defined in Eq. 1.

$$I_u = \frac{\sigma_u}{\overline{U}} \times 100, \tag{1}$$

where σ_u is the streamwise velocity standard deviation and $\overline{U}$ is the mean flow magnitude. A range of $I_u = 2$–24% in increments of 2% was applied during tests. This was sufficient to cover the range of intensities reported in the literature, which vary from 5–18% across different tidal sites in Table 1.

The other parameters were held constant with a length-scale of 10 m, 1/7th power law shear profile and a uniform standard deviation profile. A user-defined von Kármán model was used to determine the shape of the spectrum as Naberezhnykh et al. (2023b) found that the stream-wise spectra at two tidal sites were better represented by this model. A general coherence model was also applied to ensure the spatial correlation of parameters. For the tests where other parameters were varied, I_u was held constant at 10%—an approximate median of reported values in Table 1. Figure 2 shows measurements from two different sites, demonstrating the range of length-scales can occur in combination with $I_u = 10\%$.

Test 2: length-scales

Length-scales were computed by the auto-correlation method (Eq. 2), which measures the duration for which the largest eddies remain correlated (Naberezhnykh et al. 2023b) and assumes Taylor's Frozen Field hypothesis Schlipf et al. (2010):

$$R(\tau) = \frac{\langle (u_t - \overline{U})(u_{t+\tau} - \overline{U}) \rangle}{\sigma_u^2},$$
$$L_u = \overline{U} \sum_{\tau=0}^{R(\tau)=0} R(\tau) \mathrm{d}\tau, \tag{2}$$

where $R(\tau)$ is the correlation coefficient, t is time and τ is the time lag, $\overline{U}$ is the mean flow magnitude and L_u is the streamwise length-scale. Length-scales will vary by site and bathymetry; Thiébaut et al. (2020a) found L to be 2–3 times the local water depth at Alderny Race, Walter et al. (2011)

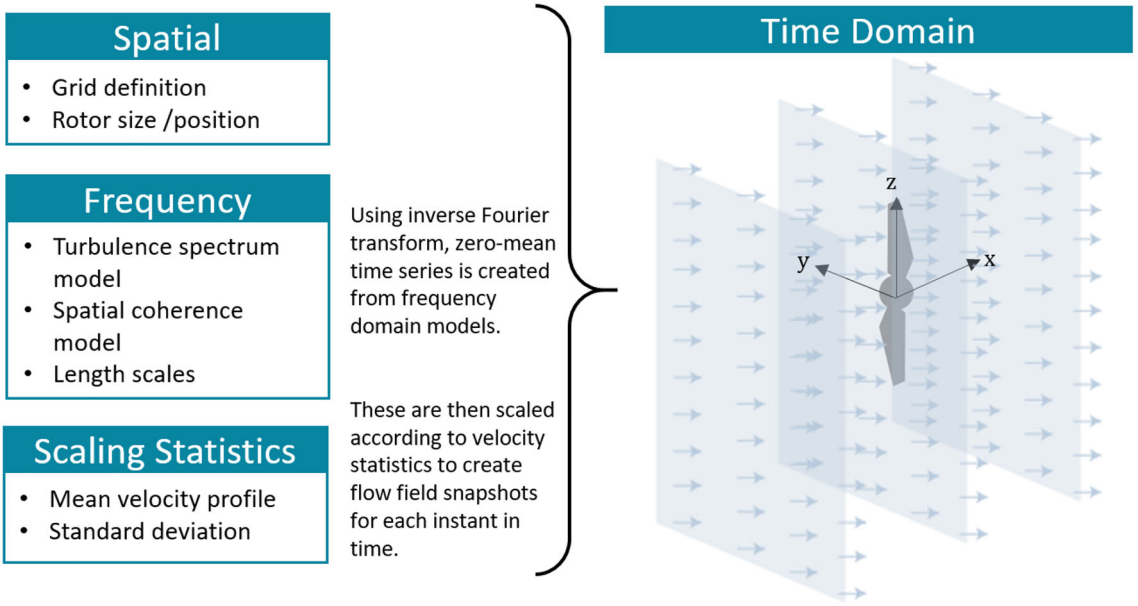

Fig. 1 Simplified illustration of the input parameters required to construct flow fields in Tidal Bladed and TurbSim. After Naberezhnykh et al. (2023b), with permissions

Table 1 Reported turbulence intensities (I_u) for various tidal sites

Location	Peak flow (m/s)	I_u (%)	z/H	References
Alderney race	4.5	17.5	0.2	Thiébaut et al. (2020b)
East river	2	13–18	0.5	Milne et al. (2016)
Puget sound	0.8–2.0	8–11	0.2	Thiebaut et al. (2020)
Sea scheldt	0.8–1.4	4–5	0.9	Thiebaut et al. (2020)
Sound of islay	2.0–2.5	11–13	0.1	Thiebaut et al. (2020)
Strangford loch	2.5–3.5	4–9	0.5	Thiebaut et al. (2020)
Fall of warness	3.7	9	0.5	Naberezhnykh et al. (2023b)
Minas basin	5.0	5–8	0.5	McMillan and Hay (2017)
Bank straits	2.0	12–17	0.2	Perez et al. (2022b)

z/H is the relative position in the water column where turbulence was measured

observed L several orders of magnitude greater than the depth at Elkhorn Slough estuary, and Milne et al. (2013) reported scales of approximately 1/3 of the channel depth at the Sound of Islay.

Length-scales and turbulence intensity are invariably linked. To ensure the test ranges represent realistic flows, we checked them against measurements from a prior study (Naberezhnykh et al. 2023b). Turbulence conditions from two test sites, Fundy Ocean Research Center for Energy (FORCE) and European Marine Energy Centre (EMEC) were found to have a broad range of length-scales and turbulence intensities (presented in Fig. 2). Across the four different measurement locations at the two sites, the length-scales can vary between 1 and 100 m for I_u range of $\approx$ 2–20%, although most of the points were concentrated below $I_u = 15\%$. Based on these measurements, the input length-scales were varied between 2 and 100 m.

For all length-scales, the generated flow turbulence intensity was held constant at 10%, and the rest of the parameters were the same as in Test 1. Although the specified range of length-scales was 2–100 m, the resulting flows had a slightly smaller range of 2–72 m. This is likely because the simulation time of 10 min is too short to capture the largest scales. Where other parameters were varied, L_u was held constant at 10 m because studies suggest that the turbulence scales that are most likely to interact with the device are similar to the blade/rotor size (Clark et al. 2015), in this case 10–20 m.

Test 3: shear profiles

According to the DNV-ST-0.164: Tidal turbines standard (DNV 2015), if site measurements are not available, the current velocity should be modelled according to power law in Eq. 3, where the exponent α is taken as $1/7$ and the velocity

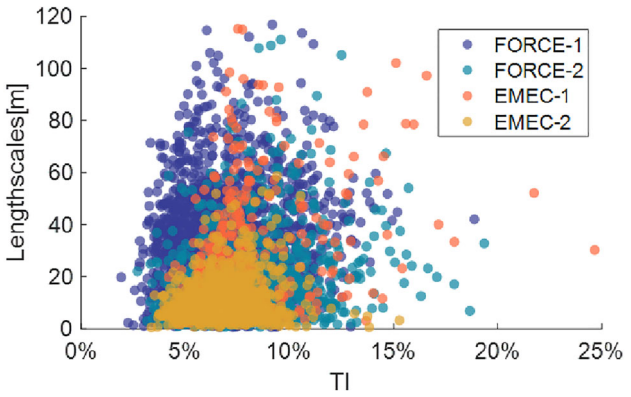

Fig. 2 Length-scales and turbulence intensity measurements from Fundy Ocean Research Centre for Energy (FORCE) and European Marine Energy centre (EMEC) tidal test sites, for details refer to Naberezhnykh et al. (2023b)

$U(z)$ at a given depth z is given by:

$$U(z) = U_{\text{ref}} \left(\frac{z}{h_{\text{ref}}} \right)^{\alpha} \quad \text{for } z \leq 0, \tag{3}$$

where U_{ref} is the reference velocity magnitude at a reference depth h_{ref}. Investigations from various tidal sites often report that the real shear profiles can deviate from this law. A number of studies (Parkinson and Collier 2016; Gunn and Stock-Williams 2013; Greenwood et al. 2019; McNaughton et al. 2013), found the shear profiles at EMEC's Fall of Warness tidal site had two distinct profile shapes, one logarithmic and one approximately polynomial. Naberezhnykh et al. (2023b) analysed profiles at various locations at two different sites and found that even when they followed a power law it often was not a 1/7th power law. Togneri and Masters (2016) analysed the velocity profiles at Ramsey Sound (Wales, UK) and reported that during ebb tides they followed the power law throughout the water depth, however, during flood tides the bottom half of the profile was logarithmic, with the upper half showing a uniform profile. Based on the findings from these studies, the test shear profiles were chosen as 1/4th, 1/7th and 1/9th power law, polynomial and uniform. For tests where parameters were varied, a 1/7th power law shear profile was applied as this profile is used by default in models.

Test 4: standard deviation profile

Although standard deviation σ_u is expected to vary with depth, models such as Tidal Bladed assume a uniform σ_u profile throughout the water column, normally scaling the turbulence according to the hub height values only (Jonkman and Kilcher 2012; Khairuzzaman 2016). Naberezhnykh et al. (2023b) presented the measured σ_u profiles from two tidal sites which were approximately linear. Based on this, two profiles were tested—uniform and linear. The rotor average σ_u was equal for both profiles to ensure we test the effect of the profile shape only. In the other tests, the default uniform standard deviation profile was applied.

Test 5: spatial coherence

Spatial coherence describes the correlation of the streamwise fluctuations across a separation distance, r, at each distinct frequency (Naberezhnykh et al. 2023b). The IEC 61400-1 (IEC 2019) wind standard describes an empirical model of streamwise coherence, which can be used alongside the Kaimal or von Kármán model spectra. Tidal Bladed and TurbSim codes both use this IEC coherence model, it is a function of frequency f, mean flow magnitude $\overline{U}$, length scales L_u and separation distance r (Naberezhnykh et al. 2023b):

$$C_u(\Delta r, f) = \exp\left(-8.8\Delta r \sqrt{\left(\frac{0.12}{L_u}\right)^2 + \left(\frac{f}{\overline{U}}\right)^2} \right). \tag{4}$$

Rather than varying the coherence model parameters, this test simply used flows with and without coherence to establish whether this has a notable impact on the loads. For all other tests, coherency was always switched on to give a more realistic flow field.

2.3 Test matrix

Table 2 summarises the five tests described in this Section. Each test was conducted for different incoming velocities; cut-in, 0.75× rated velocity, rated-velocity (where the turbine starts to exceed rated) and 1.25× rated velocity. All simulations were 10 min long with a time resolution of 10 Hz. For each test case, 30 flow iterations were produced. TurbSim randomises the occurrence and scaling of coherent events. Simulations that generate coherent turbulence time series have up to 10 degrees of stochastic freedom. The random phases associated with each frequency at each grid point and velocity component are designed to represent the expected variability in real flows. Because of the degree of variability, using 30 or more different random seeds for a specific set of conditions is recommended (Jonkman and Kilcher 2012). In total, 3720 simulations were carried out. Flow and load statistics were calculated across all flow iterations for each test.

2.4 Turbine details

The TEC used in the investigation was based on Orbital's floating O2 tidal turbine, illustrated in Fig. 3. A simplified geometry was used, with each leg of the device holding a

Table 2 Summary of the input turbulence parameter ranges tested for four different incoming velocity scenarios

Mean flow	Length scales (m)	TI (%)	Shear profile	SD profile	Coherence
> Rated (1.25 × rated)	2–100	2–24	1/4th 1/7th 1/10th polynomial uniform	Uniform Realistic	On Off
Rated	2–100	2–24	1/4th 1/7th 1/10th Polynomial Uniform	Uniform Realistic	On Off
Mid (0.75 × rated)	2–100	2–24	1/4th 1/7th 1/10th Polynomial Uniform	Uniform Realistic	On Off
Cut-in	2–100	2–24	1/4th 1/7th 1/10th Polynomial Uniform	Uniform Realistic	On Off

2-bladed 20 m rotor. Model parameters are summarised in Table 3. The details of the blade sections at each blade element were provided by and are proprietary to Orbital Marine. Platform motion aspects were intentionally excluded for simplicity. Although the tests were carried out for a floating device model, the simulation results are equally applicable to seabed turbines. All tests were run in power production mode, which means the power production control characteristics apply. The developed power and mechanical loading in flows exceeding the rated velocity are usually regulated to prevent the turbine from becoming overloaded. In this case, the device aims to maintain a constant rotational speed by controlling its blade pitch angle to suit the changing incoming velocity. Up to rated velocity, torque control is implemented, when rated velocity is exceeded, the torque is shed by pitching the blades.

2.5 Load analysis

The device loads are described in terms of thrust (T), flap-wise blade root bending moment (M_y) averages, maximums and standard deviations, as well as damage equivalent load (DEL) (see Fig. 3). For the profile tests an additional hub-bending (HB) parameter was also analysed. Details on the model algorithm used to calculate loads using BEM theory are available in the Tidal Bladed Theory Manual (Khairuzzaman 2016). Typically, loads would be described in terms of their coefficient C_t, C_{M_y} etc., which give the actual forces

Table 3 Summary of the Tidal Bladed turbine model and simulation parameters

No. of rotors	2
Rotor size	20 m
No. of blades	2
Max. rotational speed	12 RPM
Rated power	2 MW
Control system	Pitch control, variable speed
Simulation mode	Power production
Simulation time	600 s
Time step	10 Hz

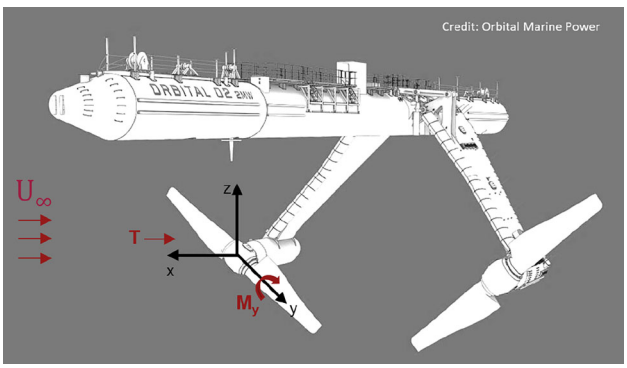

Fig. 3 Visualisation of the floating tidal turbine used in Tidal Bladed simulations with representations of the flap-wise root bending moment, M_y and thrust T forces

normalised by the total energy/force available in the flow. However, in this case we are interested in the relative effects of varying turbulence parameters so all forces are normalised by the maximum values in the test set, meaning that loads and load coefficients would yield the same result.

Fatigue load

To determine DELs, the load time series are rainflow counted. Rainflow counting is used to simplify a complex stress spectrum into a number of simpler constant amplitude cycles. Miners rule allows to account for the cumulative damage caused by each of these constant amplitude stress ranges. The rainflow counting method assumes that the bending moment cycles can be considered independently of each other and that the order they are applied does not matter (IEC 2020).

The damage equivalent load is given by the formula:

$$\mathrm{DEL} = \sqrt[m]{\frac{\Sigma l_i^m n_i}{ft}}, \tag{5}$$

where l_i is the load range of bin i, t is the length of the simulations, f is the repetition frequency, n_i is the number of rain flow cycles at stress range bin i and m is a material property given by the slope of the S–N curve for the material (Mullings and Stallard 2019). An S–N curve is a plot of the number of cycles to failure at a given cyclic load range, based on measured data from cyclic loading tests.

Load spectrum

The most important frequencies for quantifying the blade loads are likely to range from those corresponding to the integral length-scales, up to those which are equivalent to blade passing frequency (Milne et al. 2010). Turbulence slicing can be a significant source of loading as it can often generate periodic loads at the blade passing frequency, larger than those caused by the support structure shadow alone.

Load spectra are determined by applying the MATLAB function `pwelch` to each 10-min load time series. This function uses the fast Fourier transform (fft) algorithm. The time series is divided into segments and a 50% overlap is applied using a Hamming window. The resulting spectra are averaged to obtain the power spectral density (PSD) estimate (MathWorks 2023). The turbulence spectra were determined the same way by applying the function to the instantaneous velocity time series.

3 Results

3.1 Sensitivity test 1: turbulence intensity

Input flow characteristics

Figure 4 shows the turbulence parameter profiles of the flow fields for Test 1. As described in Sect. 2.2, all parameters other than turbulence intensity (and hence the standard deviation) were kept constant. Due to interactions between parameters within the model, some small variation in length-scales is present (hub height value varies between 9 and 10 m), this is considered negligible compared to the variation in turbulence intensity.

Load response

Turbulence intensity was the only test that showed an impact on the mean load quantities although it was significantly lower than for other load parameters. Up to rated velocity the variation in loads was less than 4% (Fig. 5). A load reduction up to 17% is seen at high I_u values e.g. between 15 and 25%. This is due to the turbine controller blade pitching at high velocities. The σ_T, σ_{M_y} and DEL load parameters were all found to be highly sensitive to turbulence intensity. For most velocities, the relationship is approximately linear, showing $\approx 4\%$ increase for every additional 1% in I_u for σ_T, σ_{M_y} and DEL.

Spectral analysis of both the incoming flow field and loads presented in Fig. 6a, b shows that there is a T peak at frequency equal to $2 \times$ blade passing frequency ($2P$) for mid and rated velocities, with rated showing a more prominent peak as well as another peak at $4P$. Below rated velocities, the T spectrum follows the general shape of the turbulence spectrum in the lower frequencies. As rated velocity is exceeded, the blade pitch control system sheds forces and hence the load spectrum no longer reflects the flow spectrum.

Blade root bending moments in Fig. 6c, d have acute peaks at $1P$ and $2P$. At higher turbulence intensities (e.g. $I_u = 18\%$), the peak at $2P$ is less pronounced. Similar to the T spectrum, M_y spectrum does not follow the turbulence curve above rated velocity.

3.2 Sensitivity test 2: length-scales

Input flow characteristics

Figure 7 presents the properties of the flow-fields with specified length-scales ranging 2–100 m. The largest length-scales are restricted the simulation time, so where a 100 m length-scale was specified the resulting $L = 72$ m. This still gave a reasonable range of length scales to test. Although all other parameters were held constant as described in Test 1, there

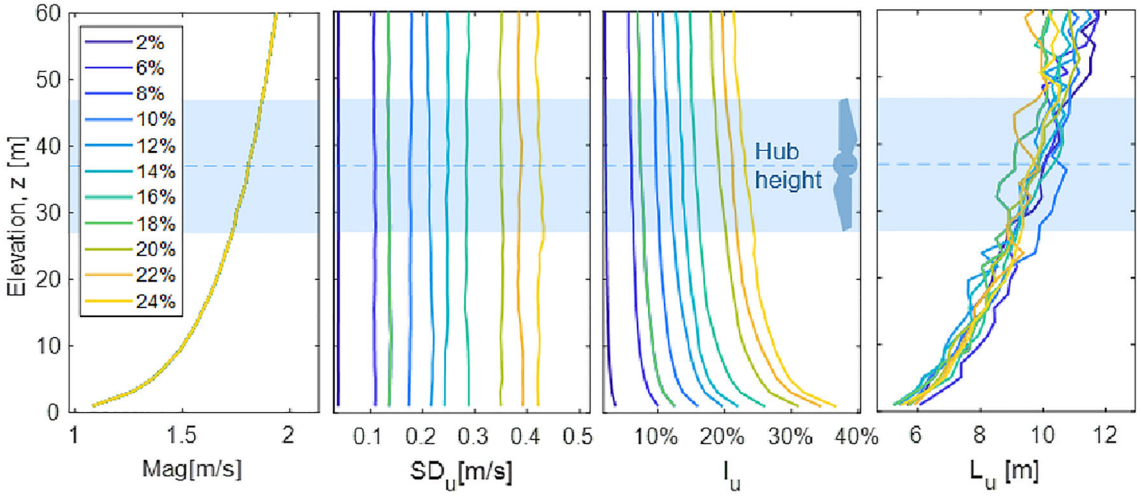

Fig. 4 Left to right: shear, standard deviation σ_u, turbulence intensity I_u and length-scale L_u profiles of TurbSim flows for Test 1—averaged over 30 flow iterations

are some small variations due to the constraints of the model. The stream-wise standard deviation has a small variation of around $\approx 5\%$ resulting in a range of TI values $\approx$ 10–11%.

Load response

The resulting mean loads showed less than 1% change between the lowest and highest length-scale tested. Load standard deviations and DELs showed a significant response to varying length-scales (Fig. 8). Both σ_T and σ_{M_y} show a maximum at $L \approx 20$ m for below-rated velocities. Between the smallest length-scale tested (2 m) and the rotor equivalent length-scale (20 m) σ_T increases by $\approx$ 20% for below-rated velocities. However, from rotor equivalent length-scale (20 m) to the largest length-scale tested (70 m) σ_T varies by less than 10%. The changes for below-rated velocities are less pronounced for σ_{M_y}. For above-rated velocities, both σ_T and σ_{M_y} show a non-linear downward trend with increasing length-scale, the same trend is seen in the $DELs$. The biggest change is seen in $DELs$ where they reduce by around 50% for above-rated velocities and 25% or above-rated between the smallest and largest length-scales.

Spectral analysis in Fig. 9a shows that at mid-velocity the load spectrum does not reflect the shape of the turbulence spectrum for the smallest (2 m) length-scales, neither is there a peak at $2P$ frequency as seen for larger length-scales. The result is similar although to a lesser extent for the 5 m length-scale test (not shown). A peak around $3P$ frequency is seen in 2 m length-scale test for rated velocity, which is not seen in larger length-scales, see Fig. 9b. The M_y spectra look similar for all length-scales at mid-velocities, Fig. 9b, with rotational sampling peaks at $1P$ and $2P$ which are higher for smaller length-scales.

Table 4 Rotor-averaged velocities for the shear profiles compared to the hub height velocity

Hub velocity (m/s)	Rotor average velocity (m/s)				
	PL4	PL7	PL10	Poly	Uni
1.10	1.10	1.10	1.10	1.09	1.10
1.80	1.81	1.80	1.80	1.78	1.80
2.50	2.51	2.50	2.50	2.47	2.50
3.00	3.01	3.01	3.00	2.96	3.00

3.3 Sensitivity test 3: shear profiles

3.3.1 Input flow characteristics

The five shear profiles are shown in Fig. 10, the mean velocity across the rotor area is consistent with the hub height value, see Table 4. As with other tests, a small variation in σ_u and L_u is present.

Load response

The mean loads did not show significant differences for varying shear profiles (Fig. 11). The maximum, standard deviation and DEL loads showed some variation but did not show a consistent response and generally did not vary by more than 10% across the tests. The exception is the result for above-rated velocities where σ_T varied by 15% between the 1/10th power-law and polynomial profiles (Fig. 12). The blade bending σ_{M_y} and DEL_{M_y} showed a more consistent response with the 1/4th power law profile resulting in the highest loads. The biggest difference was seen at rated velocity—16% change in σ_{M_y} between 1/4th power law and uniform profiles.

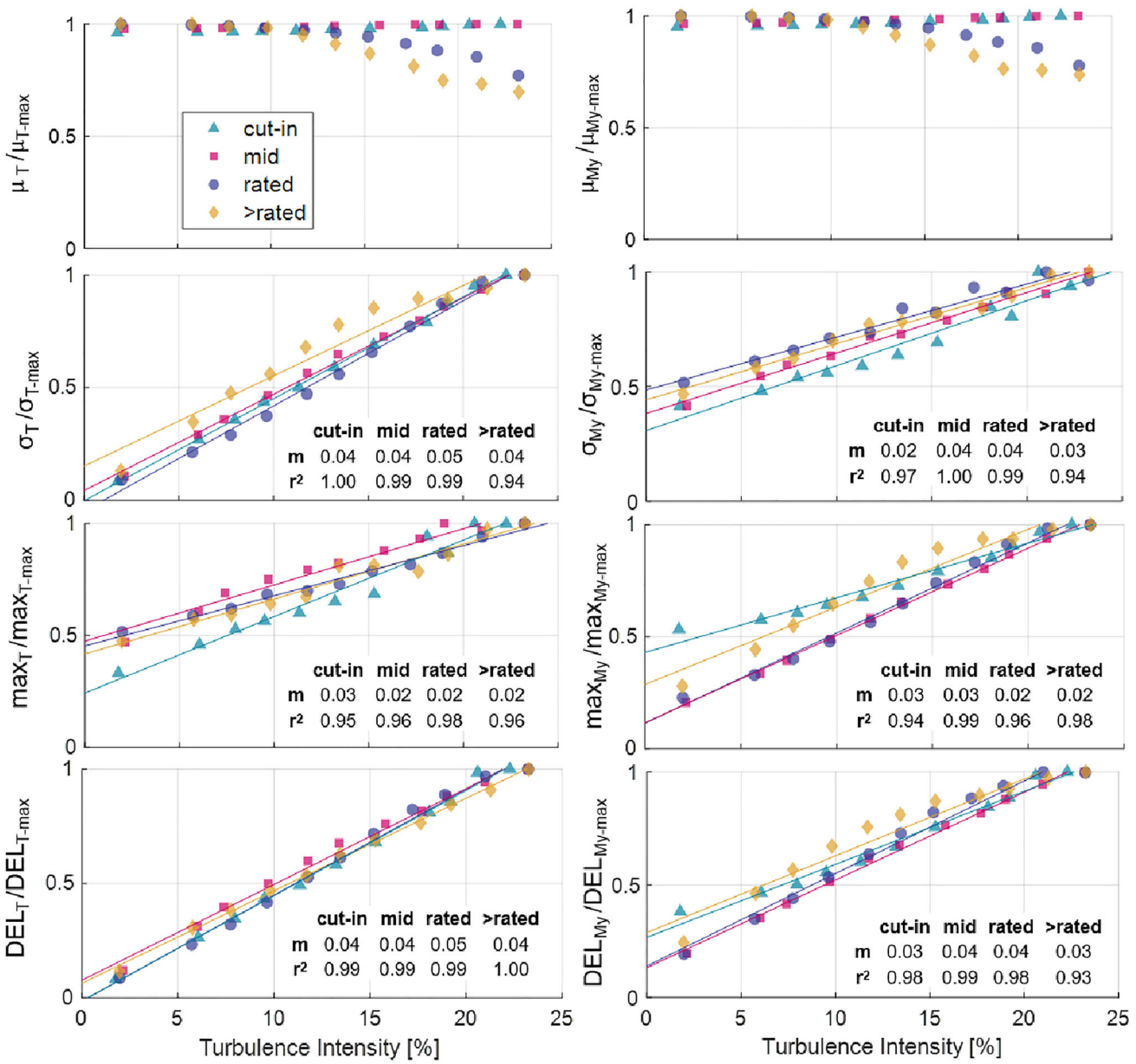

Fig. 5 Turbine response results for Test 1—turbulence intensity. Left column (top to bottom): thrust mean μ_T, standard deviation σ_T, maximum $\max_T$ and DEL. Right column (top to bottom): blade root bending moment mean μ_{M_y}, standard deviation σ_{M_y}, maximum $\max_{M_y}$ and DEL. All values are normalised by the highest value in the test set.Linear fit is provided for σ, max, and DELs with m = gradient and r^2 showing goodness of fit

The thrust spectrum looks similar for all shear profiles tested, see Fig. 13a, b. The M_y spectrum (Fig. 13c, d) has a significantly higher 1P peak for the 1/4th power law profile than for the others which is the cause for the higher M_y loads.

Figure 14 shows the additional parameters—hub-bending mean μ_{HB}, standard deviation σ_{HB}, maximum $\max_{\mathrm{HB}}$ and DEL. These show significant variations between the different shear profiles, with the 1/4th power law resulting in the highest load response—31% increase in μ_{HB} compared to the polynomial profile.

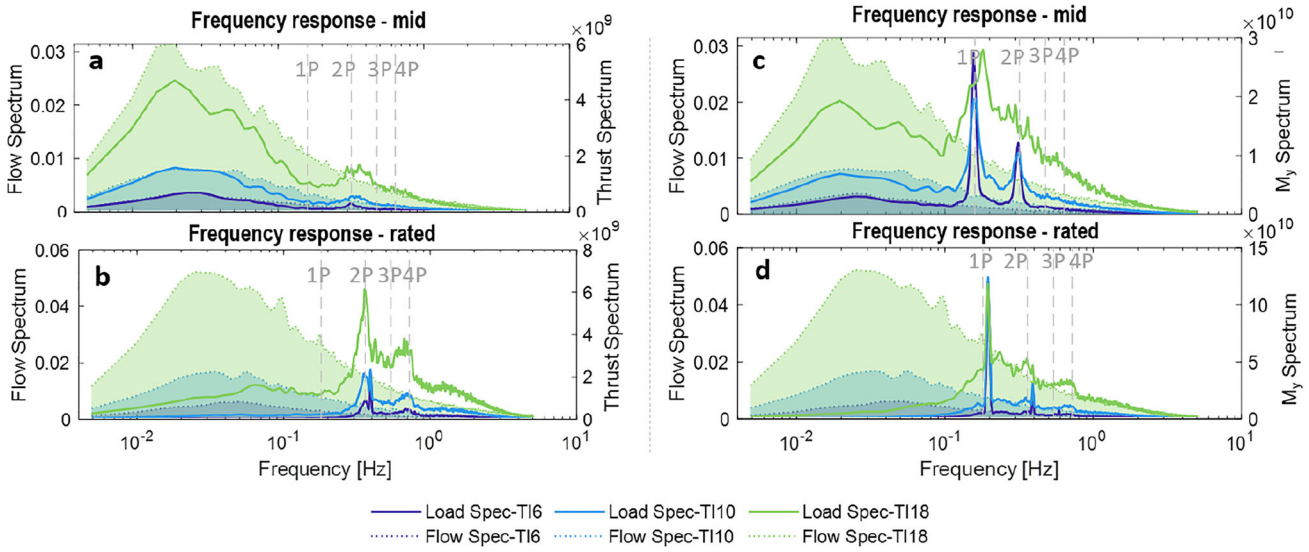

Fig. 6 Spectral analysis of the thrust T response in **a**, **b** for mid and rated velocities respectively, and blade root bending moment M_y in **c**, **d** for Test 1. The shaded areas show the turbulence spectra (left axis), the bold lines show the corresponding load spectra (right axis)

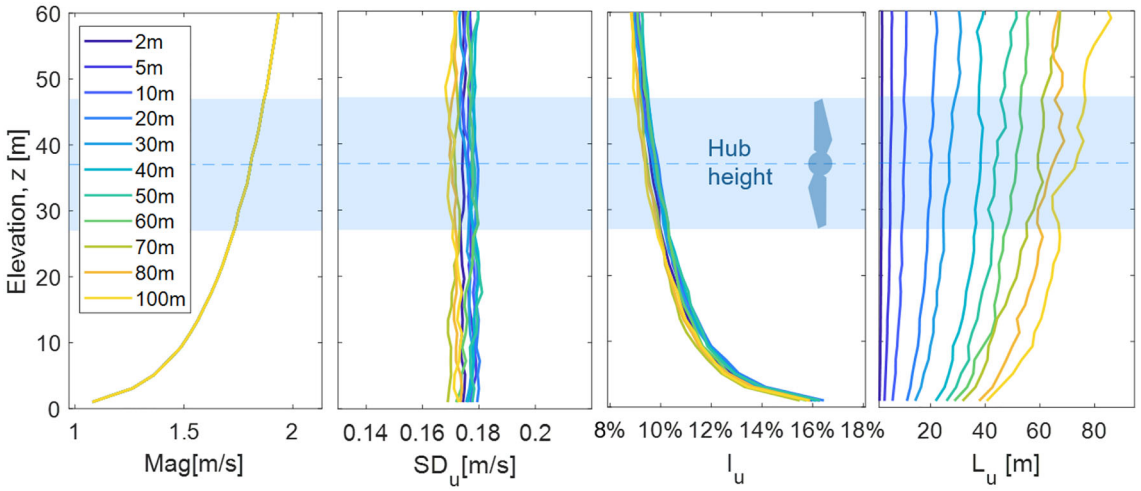

Fig. 7 Left to right: shear, standard deviation σ_u, turbulence intensity I_u and length-scale L_u profiles of TurbSim flows for Test 2—averaged over 30 flow iterations

3.4 Sensitivity test 4: standard deviation profiles

Input flow characteristics

Figure 15 shows the properties of the two profiles tested. While the profile shapes vary, the rotor-average σ_u is the same for both cases.

Load response

Similar to the other tests, very small changes were found in the mean load parameters see Fig. 16. Both σ_T and σ_{M_y} show small variations between the two profiles, with most velocities resulting in a less than 5% variation and no consistent trend. Hub bending also did not show any significant response (not shown). The biggest change—13% between the profiles was found in σ_T for above-rated velocity. Figure 17 shows that the spectral response is very similar for both cases with a very slight variation in spectral magnitudes.

3.5 Sensitivity test 5: coherence on/off

Input flow characteristics

Two types of flow field were tested; in the coherent flow field each pair of points has predefined coherence characteristics, in the non-coherent flow, fluctuations are not correlated in space. In all velocity cases, coherent flows have

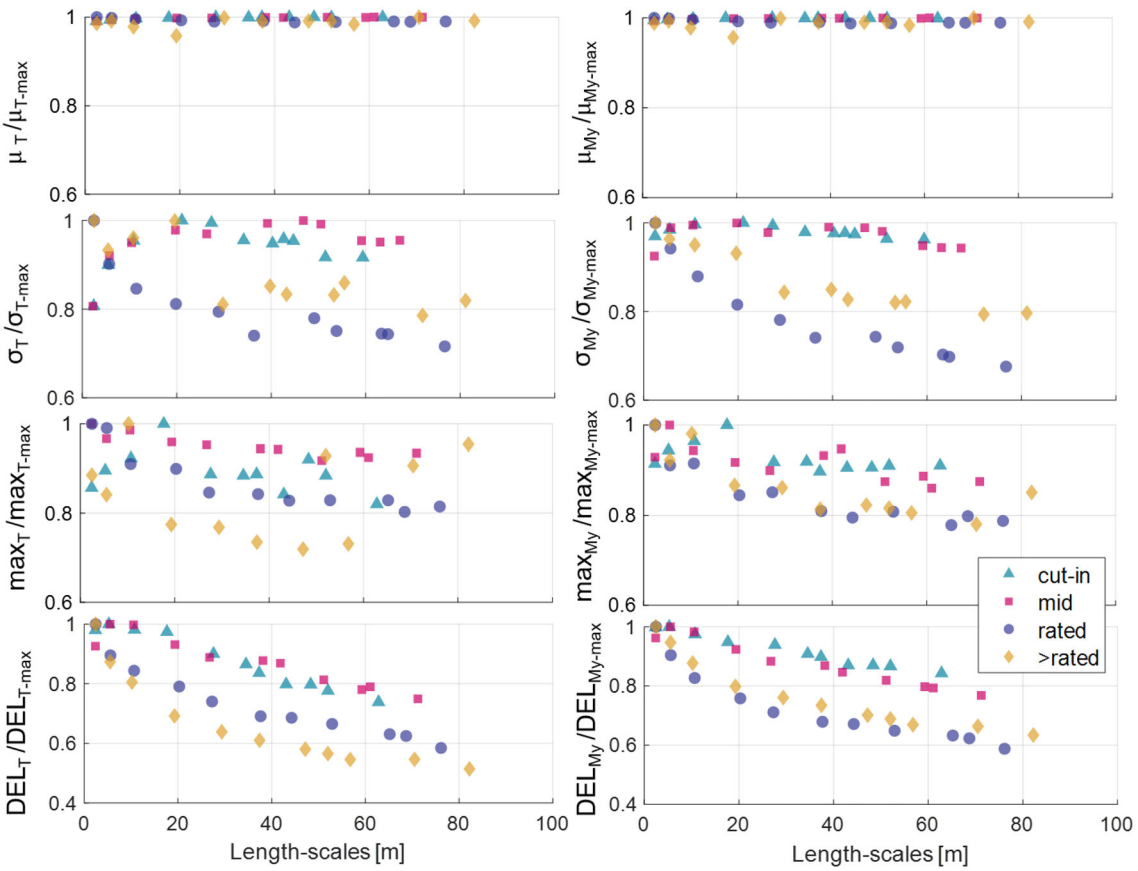

Fig. 8 Turbine response results for Test 2—length-scales. Left column (top to bottom): thrust mean μ_T, standard deviation σ_T, maximum $\max_T$ and DEL. Right column (top to bottom): blade root bending moment mean μ_{M_y}, standard deviation σ_{M_y}, maximum $\max_{M_y}$ and DEL. All values are normalised by the highest value in the test set

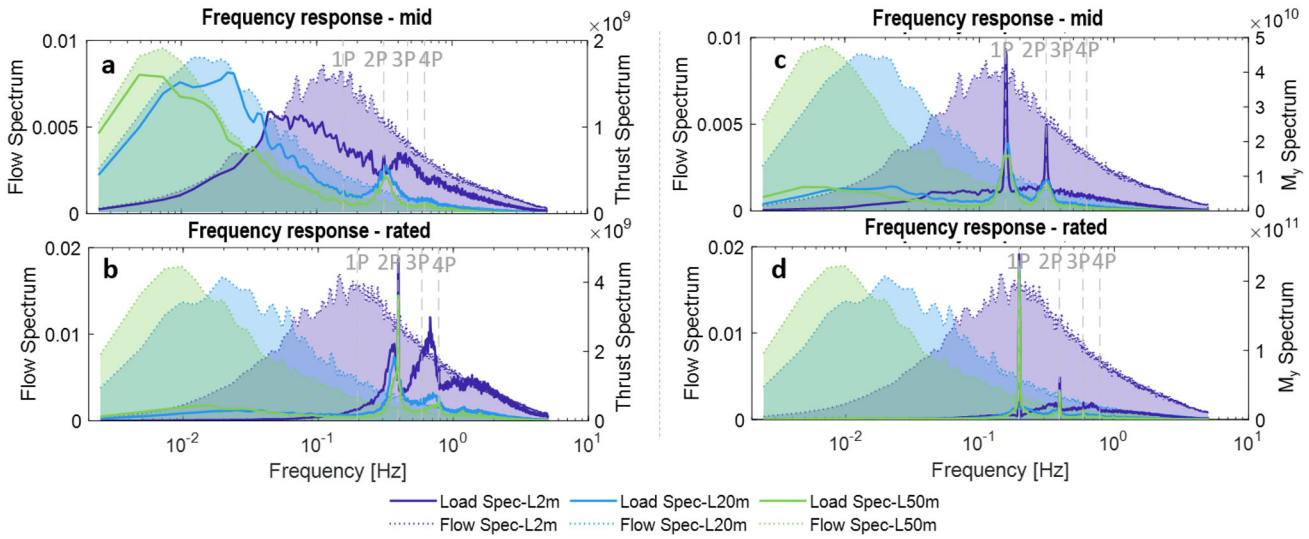

Fig. 9 Spectral analysis of the thrust T response in **a**, **b** for mid and rated velocities respectively, and blade root bending moment M_y in **c**, **d** for Test 2. The shaded areas show the turbulence spectra (left axis), the bold lines show the corresponding load spectra (right axis)

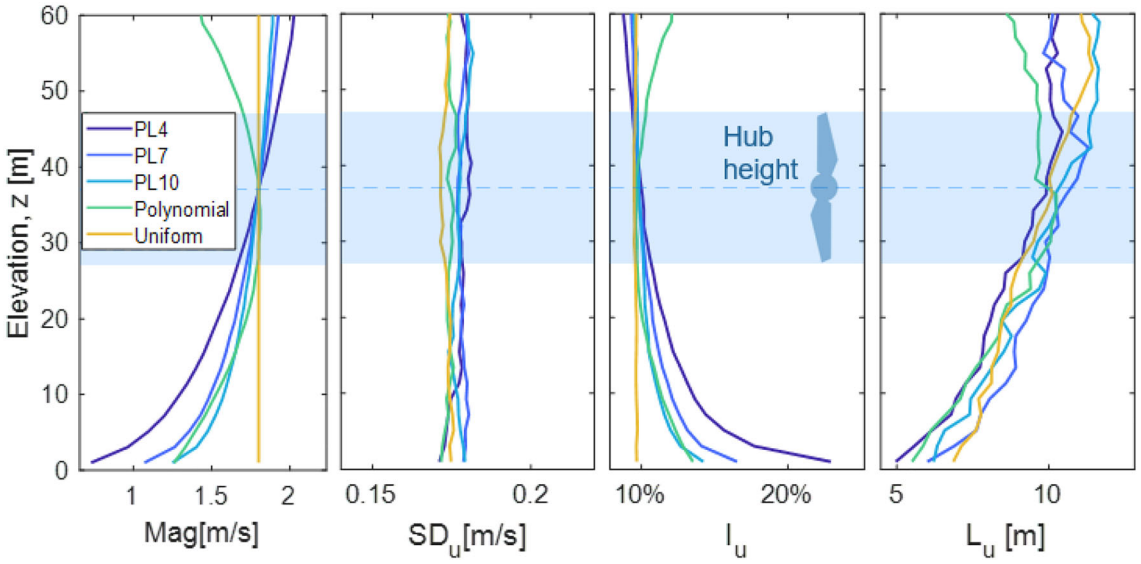

Fig. 10 Left to right: shear, standard deviation σ_u, turbulence intensity I_u and length-scale L_u profiles of TurbSim flows for Test 3—averaged over 30 flow iterations

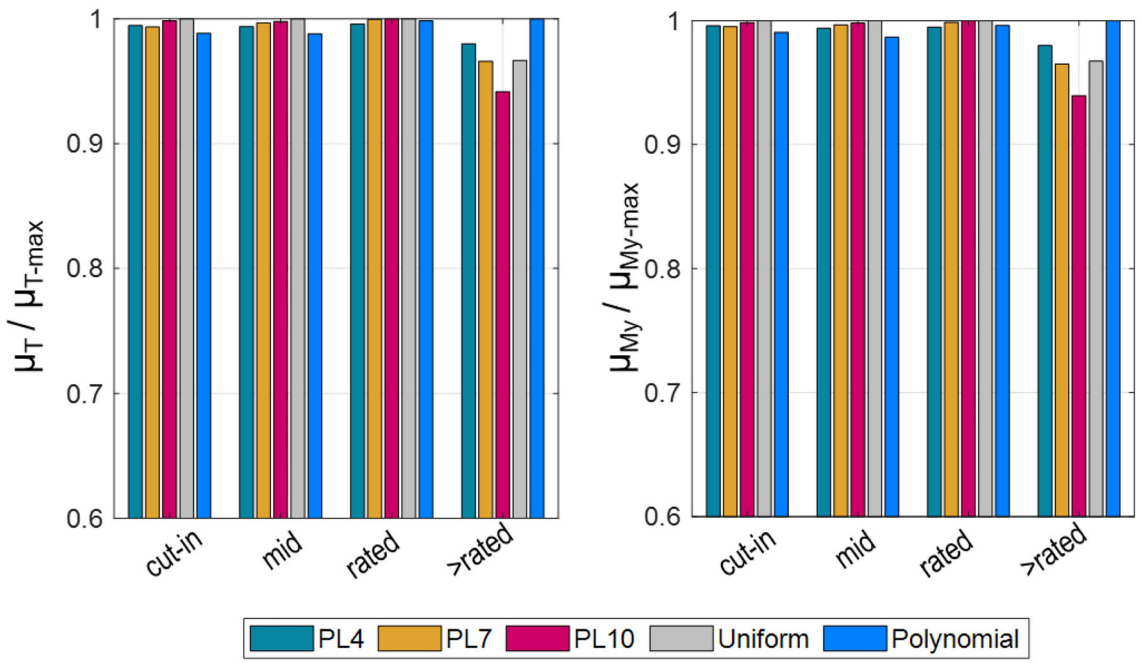

Fig. 11 Turbine mean thrust μ_T and blade root bending moment μ_{M_y} results for Test 3. All values are normalised by the highest value in the test set

a slightly higher standard deviation (2–6% increase) and the length-scales vary by 1–15% (see Fig. 18). The main difference in flow characteristics is the spatial correlation of the fluctuations. Figure 19 shows the non-coherent fluctuations are completely random and in the coherent case, they are spatially correlated, especially at lower frequencies (larger length-scales).

3.5.1 Load response

Very small changes were found in the mean load parameters. Large variations were seen in σ_T between the two cases, with coherent flows resulting in 45% load increase for below-rated velocities. A smaller but opposite effect is seen for above-rated velocities—up to 17% decrease for coherent flows. A similar but less pronounced effect is seen for σ_{M_y} maximums and $DELs$.

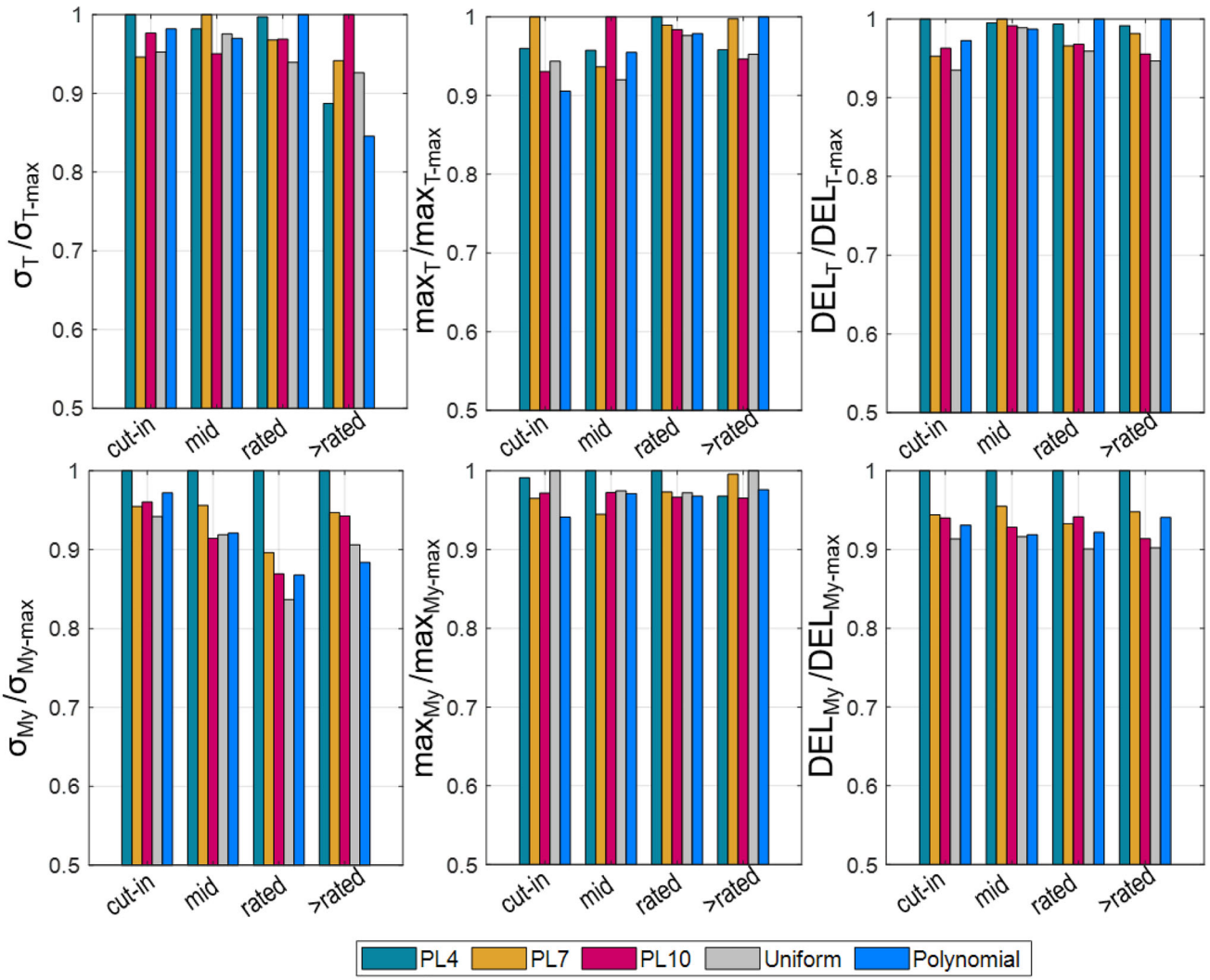

Fig. 12 Turbine response results for Test 3. Top row (left to right): thrust standard deviation σ_T, maximum $\max_T$ and DEL. Bottom row (left to right): blade root bending moment standard deviation σ_{M_y}, maximum $\max_{M_y}$ and DEL. All values are normalised by the highest value in the test set

Spectral analysis presented in Fig. 21a, b elucidates this result. During coherent flow, the thrust spectrum reflects the turbulence spectrum at mid-velocities, whereas in the non-coherent case the load spectrum does not show any response to the turbulence spectrum. Moreover, in the non-coherent case, large spikes are seen at $2P$ frequency and every harmonic thereafter. In the mid-velocity case, the coherent flow results in higher load due to the coupling of load and turbulence spectra. Above rated velocity, the high-frequency spikes dominate, resulting in non-coherent loads being higher. The same is true for σ_{M_y} and DEL, although to a lesser extent. It is worth noting the increased magnitude of the spectrum for the coherent flow. This is due to the coherence function resulting in slightly higher parameters. In the non-coherent case the load spectrum is decoupled from the flow spectrum and therefore this discrepancy is unlikely to be the driver for the results.

4 Discussion

Turbulence intensity vs length-scales

There has been some disagreement in literature on the relative importance of turbulence intensity and length-scales when it comes to turbulence-induced loads. Blackmore et al. (2016) found that loads were more sensitive to length-scales whereas other studies found more significant sensitivities to

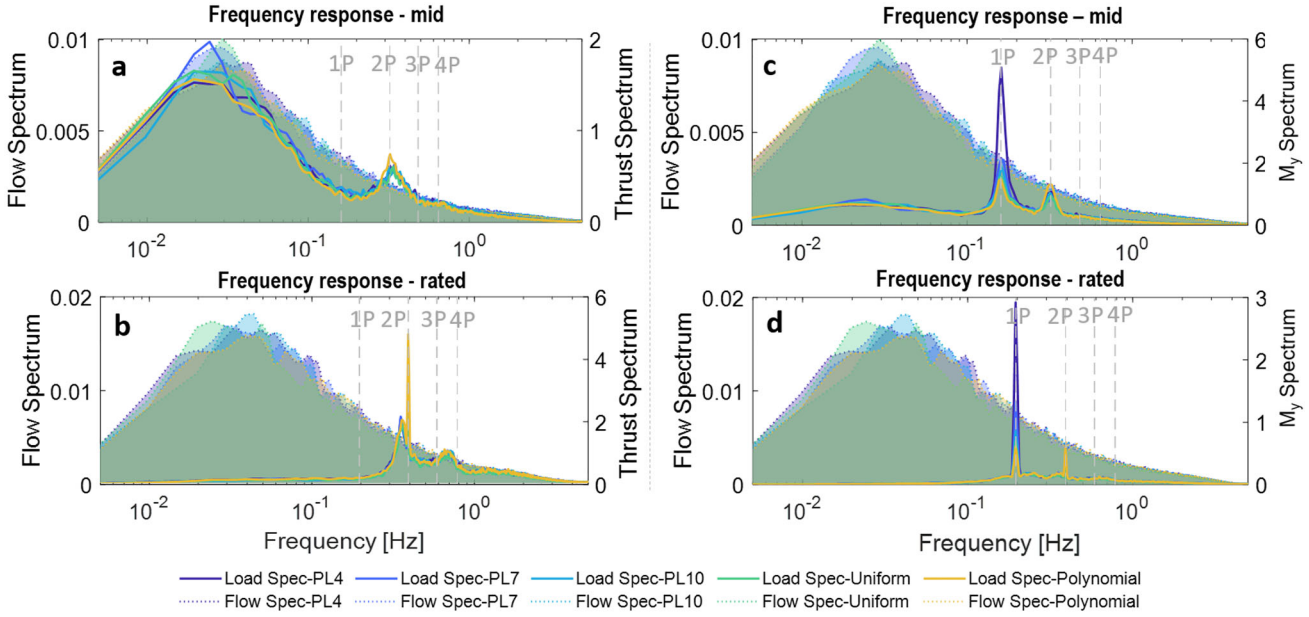

Fig. 13 Spectral analysis of the thrust T response in **a**, **b** for mid and rated velocities respectively, and blade root bending moment M_y in **c**, **d** for Test 3. The shaded areas show the turbulence spectra (left axis), the bold lines show the corresponding load spectra (right axis)

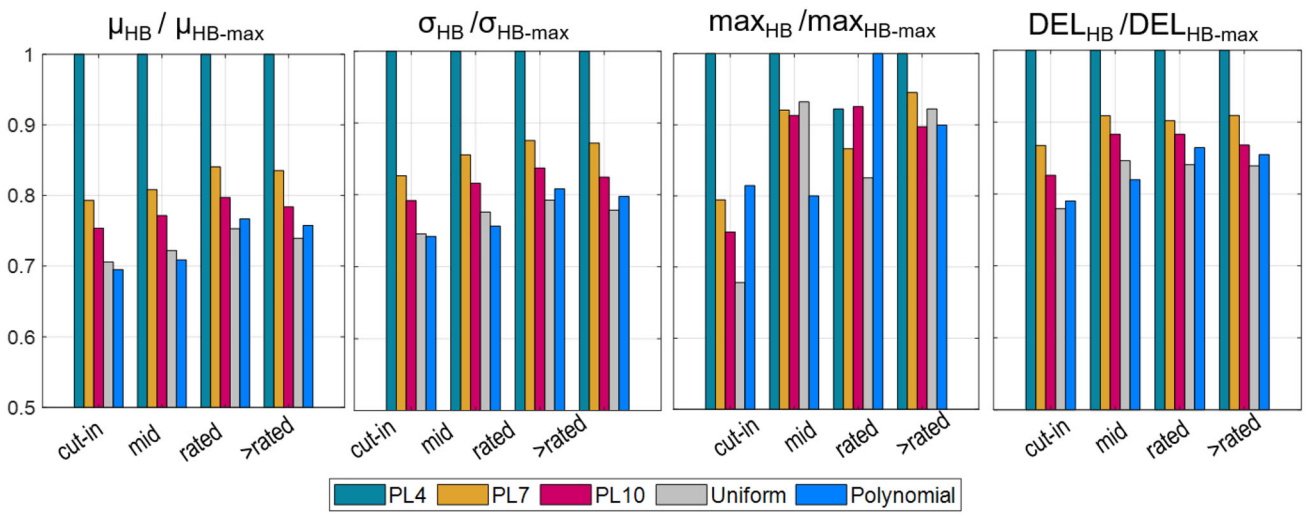

Fig. 14 Hub bending results for Test 3. Left to right: hub bending mean μ_{HB}, standard deviation σ_{HB}, maximum $\mathrm{max}_{\mathrm{HB}}$ and $\mathrm{DEL}_{\mathrm{HB}}$. All values are normalised by the highest value in the test set

turbulence intensity (Perez et al. 2022a; Milne et al. 2010; Mullings and Stallard 2021). Our study agrees with the latter, with turbulence intensity having the highest sensitivity to load standard deviations and DELs.

The relationship between I_u and σ_T, σ_{m_y} and DEL was found to be mostly linear, with a 4% increase in load quantities for every additional 1% in I_u (Fig. 5). Sellar and Sutherland (2016) showed that the presence of waves during turbulence measurements can more than double the I_u values, in particular near the top of the water column. In this situation ($I_u = 20\%$ rather than 10%), the $DELs$ could easily be overestimated by 40%. Naberezhnykh et al. (2023b) showed that instrument misalignment to the flow direction of 20° could result in I_u errors up to 30% (i.e. $I_u = 13\%$ instead of 10%), in which case the DELs would be overestimated by 12%.

Although turbulence intensity showed the highest sensitivity, other parameters also had a pronounced effect on loads. The effect of varying length-scales was most evident in the DEL results. Results show that DELs were reduced by 25% between the smallest and largest length-scales tested for below-rated velocities and by 49% for above-rated. This

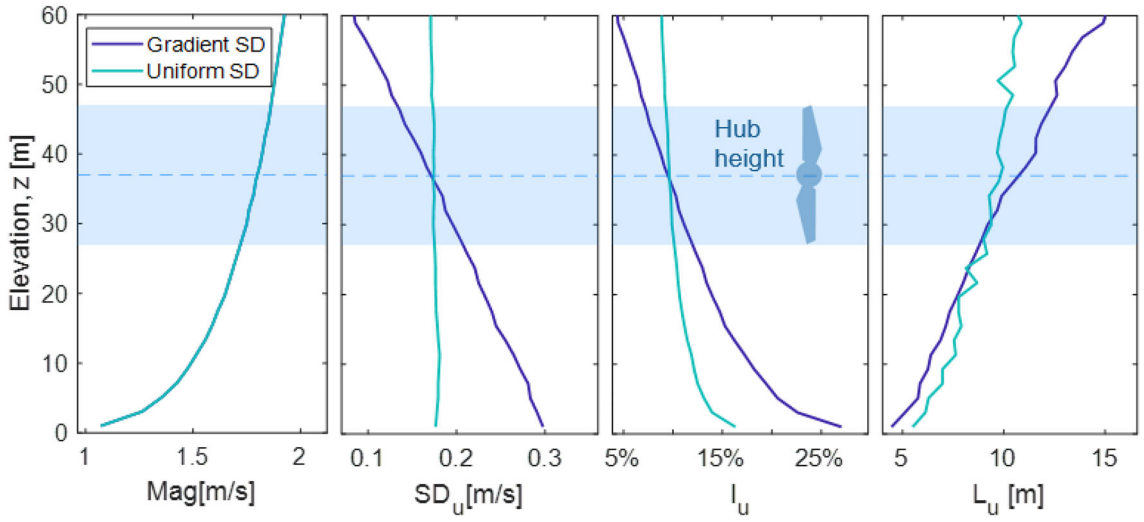

Fig. 15 Left to right: shear, standard deviation σ_u, turbulence intensity I_u and length-scale L_u profiles of TurbSim flows for Test 4—averaged over 30 flow iterations

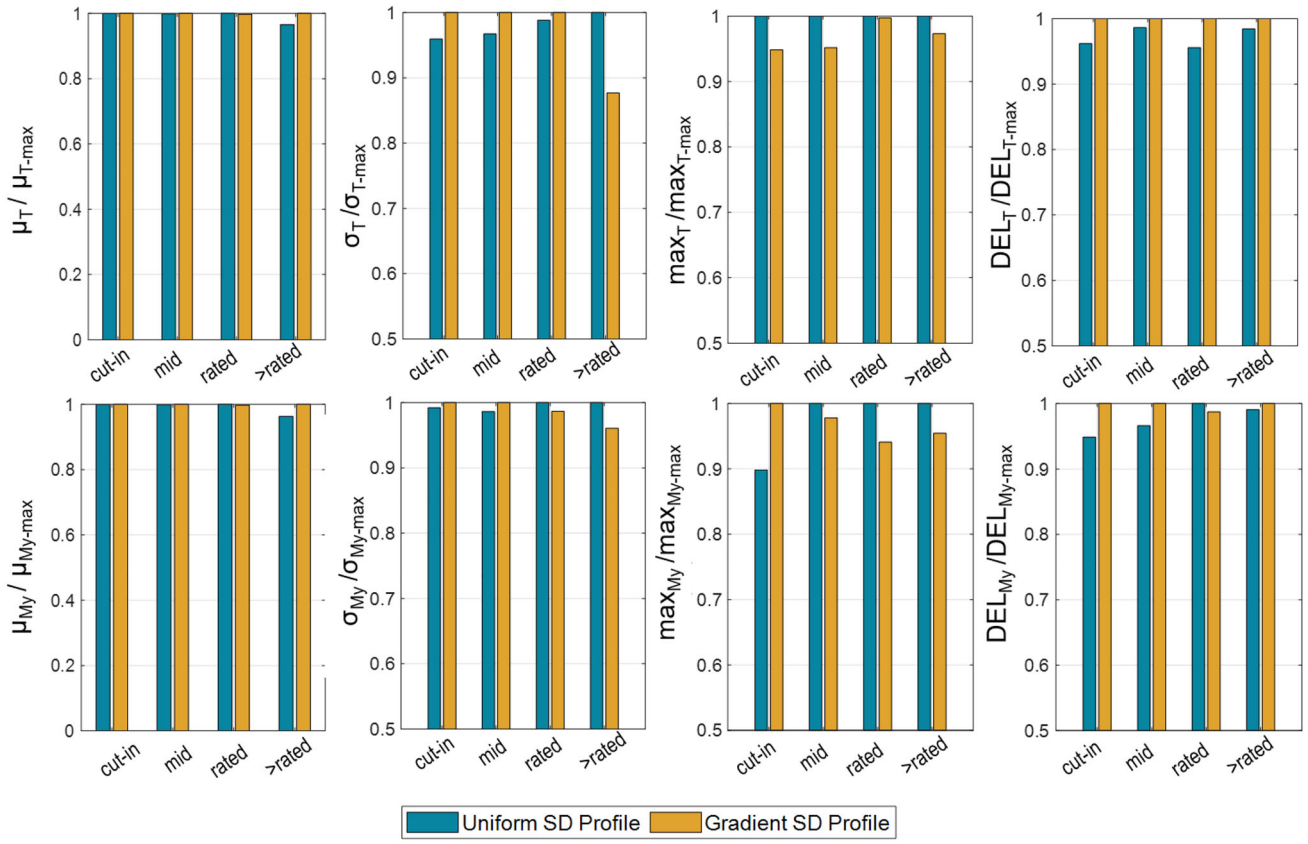

Fig. 16 Turbine response results for Test 4. Top row (left to right): thrust mean μ_T, standard deviation σ_T, maximum $\max_T$ and DEL. Bottom row (left to right): blade root bending moment mean μ_{M_y} standard deviation σ_{M_y}, maximum and DEL. All values are normalised by the highest value in the test set

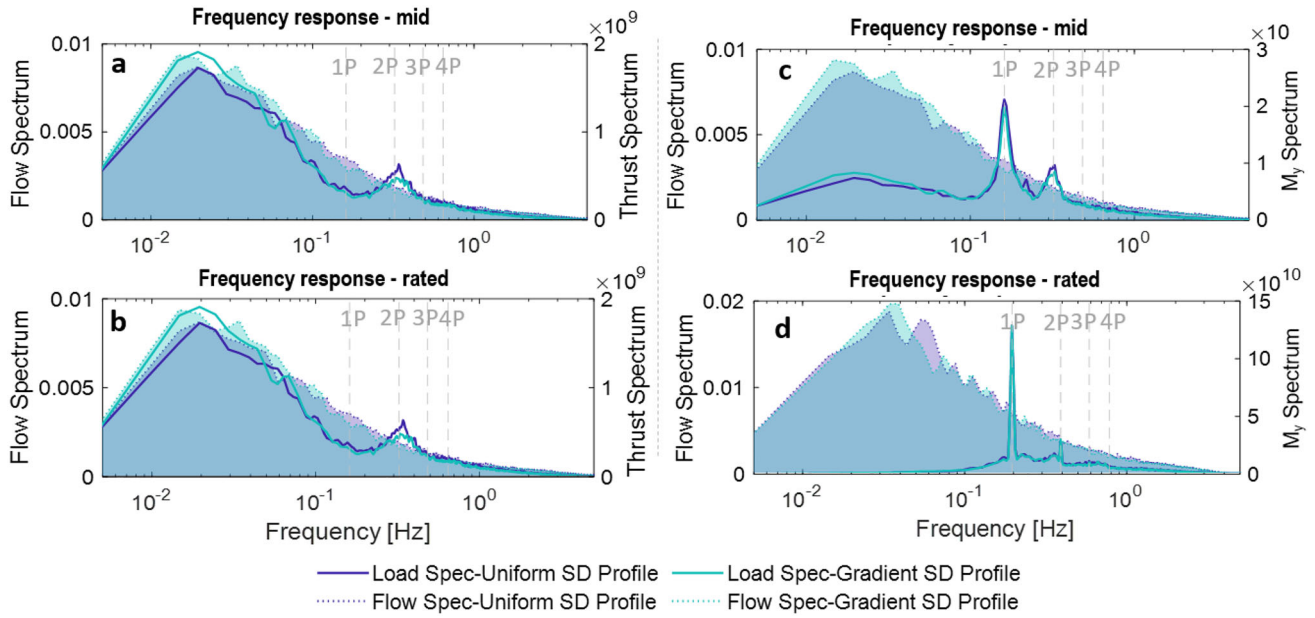

Fig. 17 Spectral analysis of the thrust T response in **a**, **b** for mid and rated velocities respectively, and blade root bending moment M_y in **c**, **d** for Test 4. The shaded areas show the turbulence spectra (left axis), the bold lines show the corresponding load spectra (right axis)

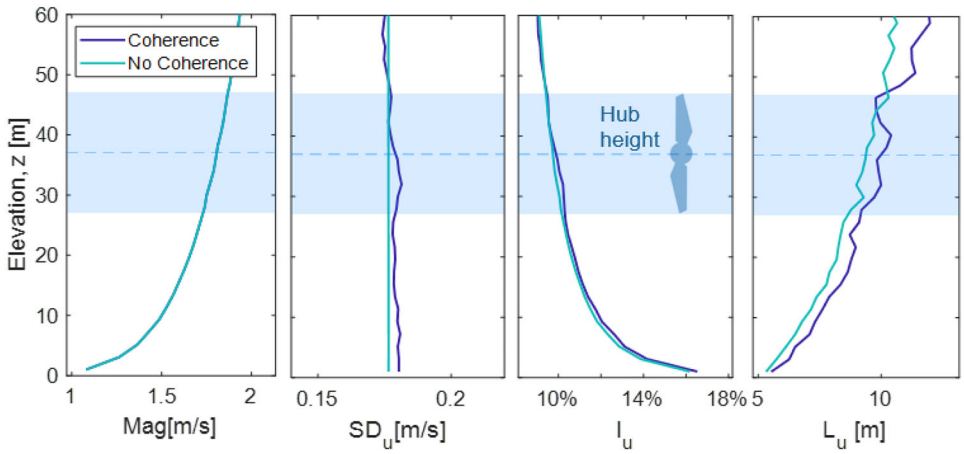

Fig. 18 Left to right: shear, standard deviation σ_u, turbulence intensity I_u and length-scale L_u profiles of TurbSim flows for Test 5—averaged over 30 flow iterations

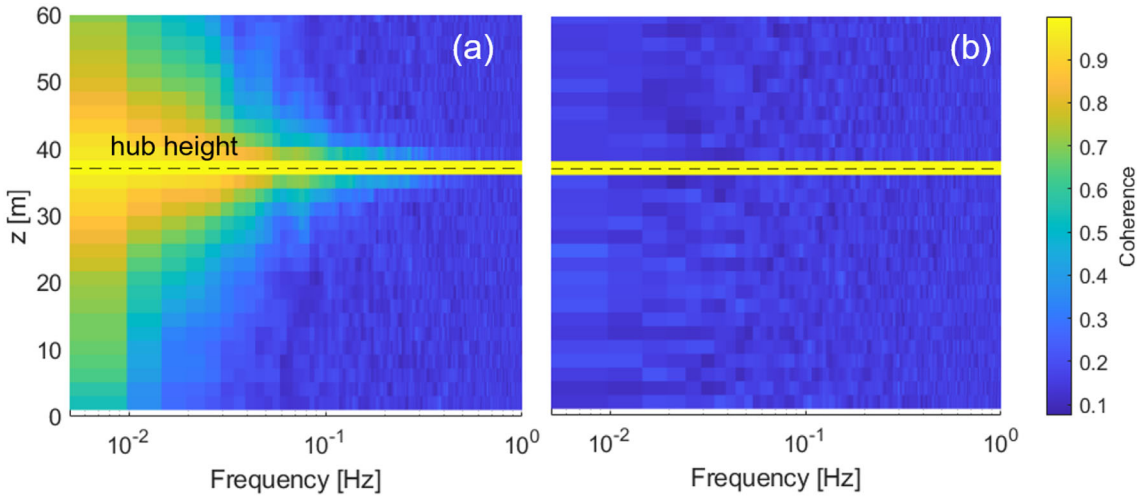

Fig. 19 Spatial coherence for the coherent (**a**) and non-coherent (**b**) flow cases

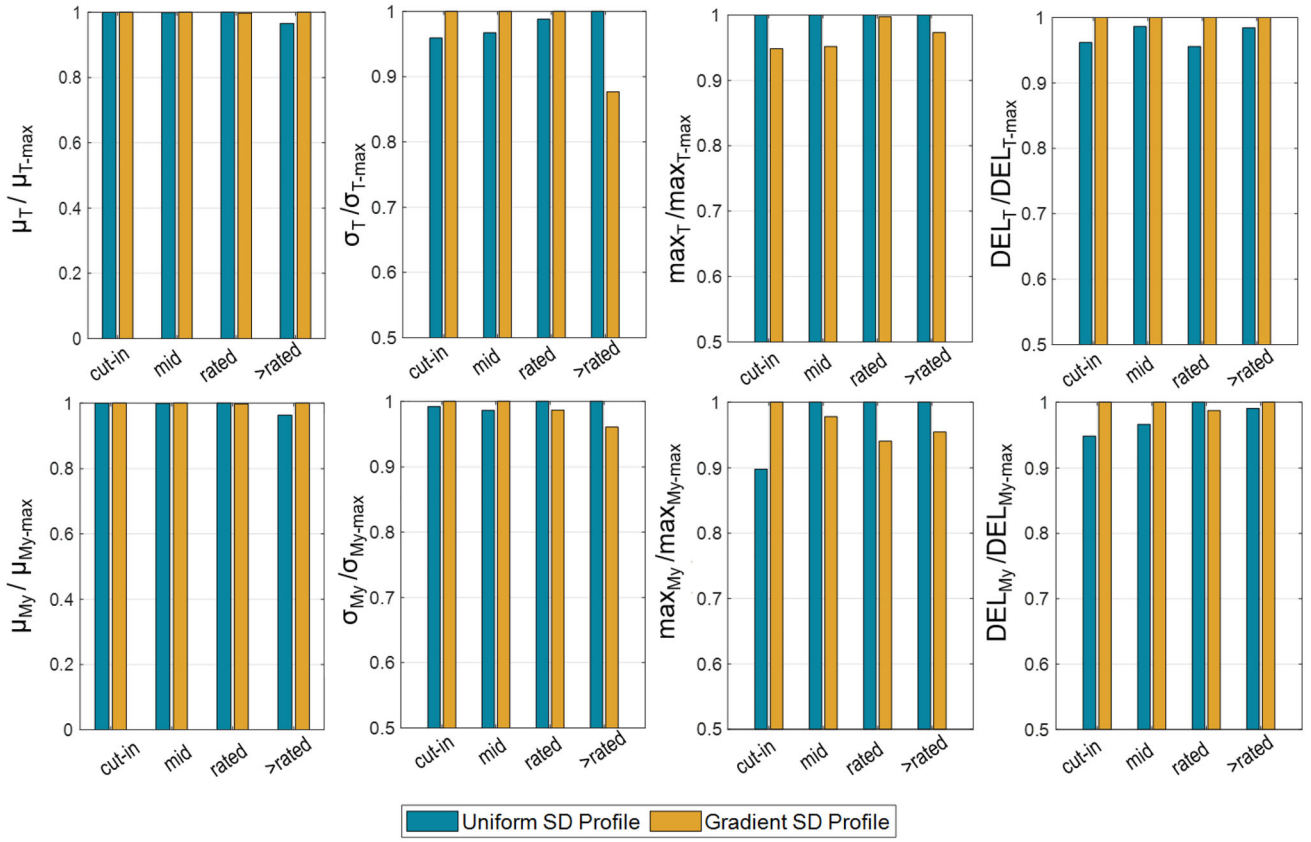

Fig. 20 Turbine response results for Test 5. Top row (left to right): thrust mean μ_T, standard deviation σ_T, maximum $\max_T$ and DEL. Bottom row (left to right): blade root bending moment mean μ_{M_y}, standard deviation σ_{M_y}, maximum and DEL. All values are normalised by the highest value in the test set

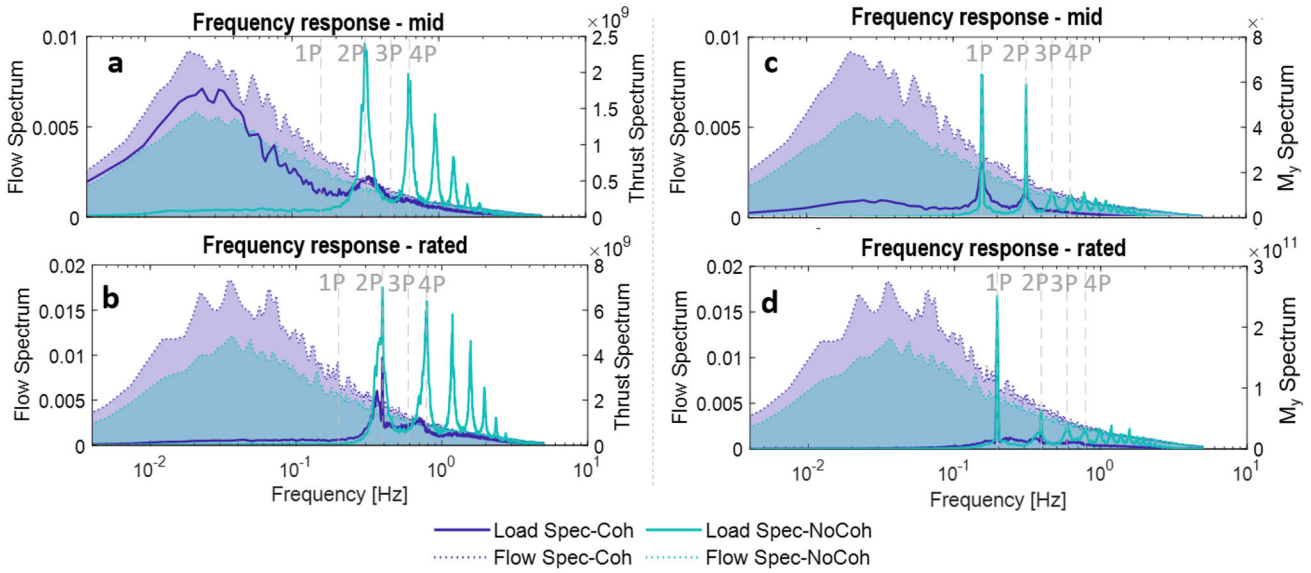

Fig. 21 Spectral analysis of the thrust T response in **a**, **b** for mid and rated velocities respectively, and blade root bending moment M_y in **c**, **d** for Test 5. The shaded areas show the turbulence spectra (left axis), the bold lines show the corresponding load spectra (right axis)

is because smaller length-scales represent higher frequency loading. In other words, if the turbulent energy is concentrated at higher frequencies, there will be more loading cycles, leading to higher fatigue loads. A maximum value of σ_T occurred at the length-scale value similar to rotor size (Fig. 8). This corresponded to a 20% increase when compared to length scales equivalent to 1/10th rotor size. The lack of response from the smallest length-scales is also evident in the spectral analysis (Fig. 9a), where for $L_u = 2$ m, the load spectrum does not reflect the turbulence spectrum and the $1P$ frequency peak does not occur like it does for larger length-scales. This is in agreement with other investigations (Blackmore et al. 2015; Sentchev et al. 2020). Naberezhnykh et al. (2023b) reported that the IEC model length-scales were up to 4 times the average measured length-scale at two tidal sites ($L_{\text{IEC}} = 113$ m vs. $L_{\text{observed}} = 30$ m). In such cases, if a theoretical value is used in modelling, it is likely to result in a DEL underestimation of $\approx 30\%$.

The importance of using realistic shear and standard deviation profiles

The biggest variation (31%) across the different shear profiles was seen in hub-bending mean and standard deviation (Fig. 14). Blade bending, σ_{M_y} varied by 16%. This result is in agreement with other studies that found a significant load sensitivity to shear profiles (McNaughton et al. 2013; Clark et al. 2015). However, our results were not as extreme as those reported by Robertson et al. (2019), who found shear sensitivities in line with turbulence intensities.

Both the blade and hub bending parameters showed the highest response to the 1/4th power law profile (Fig. 13). This is because for shear profiles, where the vertical velocity gradient within the swept area of the rotor is high, (see Fig. 10), the bending moment cycles through a larger change in amplitude every revolution of the rotor. This effect is evident in the significantly increased 1P spectral load peak for the 1/4th power law profile compared to others (Fig. 13).

A 1/7th power law is typically assumed representative of open channel flows in modelling. However, measurements often show that even when the power law applies, the exponent can vary e.g. Naberezhnykh et al. (2023b) found 1/5th power law more representative. Given that the difference in hub bending between 1/4th and 1/7th power law was found to be more than 20%, the 1/7th power law assumption is likely to result in significant inaccuracies for some sites. Assuming a 1/7th power law instead of a polynomial profile (as observed at the EMEC tidal site), could result in a 10% load overestimation, according to this study (Fig. 14).

Using a realistic standard deviation profile instead of a default uniform profile had the smallest impact on loads (Fig. 16). The load variations were inconsistent and mostly around 5%, suggesting that adding a realistic σ_u gradient into the model is less important than ensuring the other key parameters are correct.

The importance of coherence

Specifying a spatially coherent flow field increased σ_T by up to 45% for below-rated velocities (Fig. 20). Similar but slightly lower effects were seen for σ_{M_y} and DEL. When rated velocities are exceeded, the reverse relationship was observed and σ_T decreased. This is due to the coupling of the turbulence spectrum and load spectrum at low frequencies for up to rated velocities (Fig. 21), and decoupling at above-rated velocities. Using a coherence model in generating turbulent flow is essential to properly model turbine load response. In this study, coherence was simply turned on and off. In future work, different coherence curves could be investigated, to see the impact between varying levels of coherence. Naberezhnykh et al. (2023b) demonstrated that the IEC coherence model (as used in Tidal Bladed and TurbSim) was not a good representation of real flows, which could have an impact on modelled loads.

Real energetic tidal flows are non-stationary due to the presence of intermittent, energetic bursts which can have instantaneous turbulence intensities up 80% higher than the average (Naberezhnykh et al. 2023a). It is known from wind turbine field experimentation that the greatest structural fatigue damage tends to occur during such periods of coherent, turbulent bursts (Kelley et al. 2005). While some coherence (spatial correlation) is generated in stochastic models such as the ones used here, by their nature they cannot replicate non-stationary flows. Future work should investigate the effect of non-stationary coherent turbulent structures on tidal turbines. In wind, this has been done in TurbSim (used with AeroDyn) by superimposing coherent turbulent structures onto the stochastic model flows in the time domain (Kelley et al. 2005).

5 Conclusion

The aim of this study was to improve the understanding of the sensitivities of turbulence parameters in modelling turbine loads. Unlike previous work, the effects were studied by varying one parameter at a time, demonstrating the individual impacts on loads. For the first time, we also demonstrate the importance of the key input parameters relative to each other.

From the five turbulence parameters investigated, turbulence intensity showed the highest sensitivity with a 90% change in load fluctuations for the range of intensities tested ($I_u = 2$–24%). Turbulence characterisation studies have shown that Doppler noise, waves, instrument alignment as well as calculation methods all have significant impacts on

the resulting I_u value and therefore can be a significant source of inaccuracies in load modelling.

Other parameters also significantly impacted loads. Length-scales showed variations in DELs up to 49% for (L_u = 2–80 m), demonstrating that if incorrect length-scale values are used e.g. theoretical value instead of measured, the loads are unlikely to be accurately resolved.

Coherent flows resulted in loads 45% higher than non-coherent flows. Further studies should aim to understand the sensitivities of different levels of coherence and hence different coherence models. Coherence models used in Tidal Bladed and TurbSim have been shown to be poor representations of real tidal conditions and could be a source of inaccuracies in modelling.

Shear profiles had a small impact on thrust but did significantly affect blade-bending (16%) and hub-bending (30%), with the 1/4th power law profile generally resulting in the highest loads. While realistic shear profiles are important, realistic standard deviation profiles did not show a notable impact on loads and therefore the focus should be on specifying the other turbulence parameters correctly.

The findings of this study are relevant to developers and BEM model users, aiming to reduce the uncertainty in modelling. Our results show that variations in key turbulence input parameters can have profound impacts on the modelled loads, which can lead to high uncertainty and conservatism in design. This study highlights the importance of using site measurements and appropriate techniques to calculate turbulence intensity and length-scales, as well as using realistic profiles and coherence when modelling turbulence-induced loads.

Acknowledgements The authors wish to thank Mark Byers from Orbital Marine for his support and guidance on Tidal Bladed modelling and model configuration.

Author contribution Conceptualization, AN, DI, IA and CM; methodology, AN, DI, IA; software, AN; validation, AN, DI and CM; formal analysis, AN; investigation, AN; resources, CM; data curation, AN; writing-original draft preparation, AN; writing-review and editing, AN, DI, IA and CM; visualization, AN; supervision, DI and IA; All authors have read and agreed to the published version of the manuscript.

Funding This work was funded as part of the EPSRC and NERC Industrial Centre for Doctoral Training in Offshore Renewable Energy (IDCORE), Grant number EP/S023933/1.

Availability of data and materials 3rd Party Data. Restrictions apply to the availability of the data used in this study. Data was obtained from the European Marine Energy Centre and Orbital Marine Power.

Declarations

Conflict of interest The authors declare no conflicts of interest associated with this publication, and there has been no significant financial support for this work that could have influenced its outcome.

Ethics approval Not applicable.

Open Access This article is licensed under a Creative Commons Attribution 4.0 International License, which permits use, sharing, adaptation, distribution and reproduction in any medium or format, as long as you give appropriate credit to the original author(s) and the source, provide a link to the Creative Commons licence, and indicate if changes were made. The images or other third party material in this article are included in the article's Creative Commons licence, unless indicated otherwise in a credit line to the material. If material is not included in the article's Creative Commons licence and your intended use is not permitted by statutory regulation or exceeds the permitted use, you will need to obtain permission directly from the copyright holder. To view a copy of this licence, visit http://creativecommons.org/licenses/by/4.0/.

References

Blackmore T, Gaurier B, Myers L, Germain G, Bahaj AS (2015) The effect of freestream turbulence on tidal turbines. In: Proceedings of the 11th European wave and tidal energy conference, vol 585, Nantes, France, September 2015 https://www.researchgate.net/publication/282807576. Accessed 20 Feb 2023

Blackmore T, Myers LE, Bahaj AS (2016) Effects of turbulence on tidal turbines: implications to performance, blade loads, and condition monitoring. Int J Mar Energy 14:1–26. https://doi.org/10.1016/j.ijome.2016.04.017

Clark T, Roc T, Fisher S, Minn N (2015) Part 3: Turbulence and turbulent effects in turbine array engineering. Turbulence: Best Practises for the Tidal Power Industry. Carbon Trust. Doc No. MRCF-TiME-KS10

DESNZ (2023) Department for Energy Security and Net Zero, UK Government, Outcome of Contracts For Difference (CfD) Allocation Round 5 which Commenced on 30 March 2023. Contracts For Difference (CFD) Allocation Round 5: Results. https://www.gov.uk/government/publications/contracts-for-difference-cfd-allocation-round-5-results. Accessed 10 Oct 2023

DNV (2015) DNV-ST-0164: tidal turbines, edition October 2015

DNV (2023) Tidal bladed software. DNV. www.dnv.com/services/industry-standard-tidal-turbine-software-modelling-tool-tidalbladed-3799. Accessed 20 Feb 2023

El-Shahat SA, Li G, Lai F, Fu L (2020) Investigation of parameters affecting horizontal axis tidal current turbines modeling by blade element momentum theory. Ocean Eng 202(107):176. https://doi.org/10.1016/j.oceaneng.2020.107176

Frost C (2022) Cost reduction pathway of tidal stream energy in the UK and France. TIGER Project, 2023, p 2022. https://interregtiger.com/download/tiger-report-cost-reduction-pathway/. Accessed 29 Nov 2023

Greenwood C, Vogler A, Venugopal V (2019) On the variation of turbulence in a high-velocity tidal channel. Energies 12(4):672. https://doi.org/10.3390/en12040672

Gunn K, Stock-Williams C (2013) On validating numerical hydrodynamic models of complex tidal flow. Int J Mar Energy. https://doi.org/10.1016/j.ijome.2013.11.013

Hu W, Letson F, Barthelmie RJ, Pryor SC (2018) Wind gust characterization at wind turbine relevant heights in moderately complex terrain. J Appl Meteorol Climatol 57:1459–1476. https://doi.org/10.1175/JAMC-D-18-0040.1

IEC 61400-1:2019 (2019) BSI standards publication. Wind energy generation systems - Part 1: Design requirements

International Electrotechnical Commission (2020) IEC TS 62600-3: 2020. BSI tandards publication. Marine energy-wave, tidal and other water current converters. https://webstore.iec.ch/publication/60359. Accessed 28 Nov 2023

Jonkman B, Kilcher L (2012) TurbSim user's guide: version 2.00.00. National Renewable Energy Laboratory, Golden, CO, USA. https://www.nrel.gov/wind/nwtc/assets/downloads/TurbSim/TurbSim_v2.00.pdf. Accessed 28 Nov 2023

Kelley ND, Jonkman BJ, Scott GN, Bialasiewicz JT, Redmond LS (2005) Impact of coherent turbulence on wind turbine aeroelastic response and its simulation (No. NREL/CP-500-38074). National Renewable Energy Lab. (NREL), Golden, CO. http://www.nrel.gov/docs/fy05osti/38074.pdf. Accessed 20 Feb 2023

Khairuzzaman MQ (2016) Tidal Bladed theory manual. DNV-GL Energy. Version 4.8

MathWorks (2023) Welch's power spectral density estimate function, Signal Processing Toolbox, Matlab Documentation, Mathworks. https://uk.mathworks.com/help/signal/ref/pwelch.html. Accessed 20 Feb 2023

McMillan JM, Hay AE (2017) Spectral and structure function estimates of turbulence dissipation rates in a high-flow tidal channel using broadband adcps. J Atmos Ocean Technol 34:5–20. https://doi.org/10.1175/JTECH-D-16-0131.1

McNaughton J, Rolfo S, Apsley DD, Stallard T, Stansby PK (2013) Cfd power and load prediction on a 1mw tidal stream turbine. In: Proceedings of the 10th European wave and tidal energy conference, Aalborg, Denmark

Milne IA, Sharma RN, Flay RG, Bickerton S (2010) The role of onset turbulence on tidal turbine blade loads. In: 17th Australasian fluid mechanics conference, Auckland, New Zealand, pp 444–447

Milne IA, Sharma RN, Flay RG, Bickerton S (2013) Characteristics of the turbulence in the flow at a tidal stream power site. Philos Trans R Soc A Math Phys Eng Sci. https://doi.org/10.1098/rsta.2012.0196

Milne IA, Day AH, Sharma RN, Flay RG (2016) The characterisation of the hydrodynamic loads on tidal turbines due to turbulence. Renew Sustain Energy Rev 56:851–864. https://doi.org/10.1016/j.rser.2015.11.095

Mullings H, Stallard T (2019) Unsteady loading in a tidal array due to simulated turbulent onset flow. In: Advances in renewable energies offshore—proceedings of the 3rd international conference on renewable energies offshore, RENEW 2018, Lisbon, Portugal, pp 227–235

Mullings H, Stallard T (2021) Assessment of dependency of unsteady onset flow and resultant tidal turbine fatigue loads on measurement position at a tidal site. Energies 14(17):5470. https://doi.org/10.3390/en14175470

Mycek P, Gaurier B, Germain G, Pinon G, Rivoalen E (2014) Experimental study of the turbulence intensity effects on marine current turbines behaviour. Part I: one single turbine. Renew Energy 66:729–746. https://doi.org/10.1016/j.renene.2013.12.036

Naberezhnykh A, Ingram D, Ashton I (2023) Wavelet applications for turbulence characterisation of real tidal flows measured with an ADCP. Ocean Eng 270:113616. https://doi.org/10.1016/j.oceaneng.2022.113616

Naberezhnykh A, Ingram D, Ashton I, Culina J (2023) How applicable are turbulence assumptions used in the tidal energy industry? Energies 16(4):1881. https://doi.org/10.3390/en16041881

Nevalainen TM, Johnstone CM, Grant AD (2016) A sensitivity analysis on tidal stream turbine loads caused by operational, geometric design and inflow parameters. Int J Mar Energy 16:51–64. https://doi.org/10.1016/j.ijome.2016.05.005

NREL (2023) Turbsim Software v.2.00, Data and Tools, Wind Research, NREL. https://www.nrel.gov/wind/nwtc/turbsim.html. Accessed 20 Feb 2023

Ortega A, Tomy JP, Shek J, Paboeuf S, Ingram D (2020) An intercomparison of dynamic, fully coupled, electro-mechanical, models of tidal turbines. Energies 13(20):5389. https://doi.org/10.3390/en13205389

Parkinson SG, Collier WJ (2016) Model validation of hydrodynamic loads and performance of a full-scale tidal turbine using tidal bladed. Int J Mar Energy 16:279–297. https://doi.org/10.1016/j.ijome.2016.08.001

Perez L, Cossu R, Couzi C, Penesis I (2020) Wave-turbulence decomposition methods applied to tidal energy site assessment. Energies 13(5):1245. https://doi.org/10.3390/en13051245

Perez L, Cossu R, Grinham A, Penesis I (2022) An investigation of tidal turbine performance and loads under various turbulence conditions using blade element momentum theory and high-frequency field data acquired in two prospective tidal energy sites in australia. Renew Energy 201:928–937. https://doi.org/10.1016/j.renene.2022.11.019

Perez L, Cossu R, Grinham A, Penesis I (2022) Tidal turbine performance and loads for various hub heights and wave conditions using high-frequency field measurements and blade element momentum theory. Renew Energy 200:1548–1560. https://doi.org/10.1016/j.renene.2022.10.058

Robertson AN, Sethuraman L, Jonkman J, Quick J (2019) Assessment of wind parameter sensitivity on ultimate and fatigue wind turbine loads. In: AIAA Scitech 2019 Forum, San Diego, California, https://doi.org/10.2514/6.2019-0248

Scarlett GT, Viola IM (2020) Unsteady hydrodynamics of tidal turbine blades. Renew Energy 146:843–855. https://doi.org/10.1016/j.renene.2019.06.153

Schlipf D, Trabucchi D, Bischoff O (2010) Testing of frozen turbulence hypothesis for wind turbine applications with a scanning lidar system. Geophys Res Abstr 12:5410

Sellar BG, Sutherland DR (2016) Tidal energy site characterisation at the Fall of Warness, EMEC, UK. Energy Technologies Institute REDAPT MA1001 (MD3. 8), Institute for Energy Systems, School of Engineering, University of Edinburgh. http://redapt.eng.ed.ac.uk. Accessed 20 Feb 2023

Sentchev A, Thiébaut M, Schmitt FG (2020) Impact of turbulence on power production by a free-stream tidal turbine in real sea conditions. Renew Energy 147:1932–1940. https://doi.org/10.1016/j.renene.2019.09.136

Smyth M (2019) Three-dimensional unsteady hydrodynamics of tidal turbines. PhD Dissertation, University of Cambridge

Thiebaut M, Filipot JF, Maisondieu C, Damblans G, Jochum C, Kilcher LF, Guillou S (2020) Characterization of the vertical evolution of the three-dimensional turbulence for fatigue design of tidal turbines. Philos Trans R Soc A 378(2178):20190495

Thiébaut M, Filipot JF, Maisondieu C, Damblans G, Duarte R, Droniou E, Chaplain N, Guillou S (2020) A comprehensive assessment of turbulence at a tidal-stream energy site influenced by wind-generated ocean waves. Energy 191:116550. https://doi.org/10.1016/j.energy.2019.116550

Thiébaut M, Filipot JF, Maisondieu C, Damblans G, Duarte R, Droniou E, Guillou S (2020) Assessing the turbulent kinetic energy budget in an energetic tidal flow from measurements of coupled ADCPs. Philos Trans R Soc A 378(2178):20190496. https://doi.org/10.1098/rsta.2019.0496

Togneri M, Masters I (2016) Micrositing variability and mean flow scaling for marine turbulence in Ramsey sound. J Ocean Eng Mar Energy 2:35–46. https://doi.org/10.1007/s40722-015-0036-0

Veers PS (1988) Three-dimensional wind simulation. No. SAND-88-0152C; CONF-890102-9. Sandia National Labs., Albuquerque, NM, USA

Walter RK, Nidzieko NJ, Monismith SG (2011) Similarity scaling of turbulence spectra and cospectra in a shallow tidal flow. J Geophys Res Oceans 116:1–14. https://doi.org/10.1029/2011JC007144

Publisher's Note Springer Nature remains neutral with regard to jurisdictional claims in published maps and institutional affiliations.